collection. Our data show, however, that there is also a "background" source of <190°C group H5 chondrites (for example, Fig. 1), with cosmic-ray exposure ages of >20 Ma, which might represent earlier breakup events or even fragments of a completely different parent body.

In summary, we suggest that we can now account for the origin and destruction of a large group of H5 chondrites found only in the Antarctic meteorite collection. Our data show that the terrestrial meteorite flux is not a constant. Numbers, sizes, and relative proportions of different meteorite types can change over relatively short periods of time, at least in some cases. In this light, we suggest that a more critical examination of the large Antarctic meteorite collection may well turn up more cases of temporal changes in the meteorite flux.

REFERENCES AND NOTES

1. I. M. Whillans and W. A. Cassidy, *Science* **222**, 55 (1983).
2. J. T. Wasson, *Meteorites: Their Record of Early Solar-System History* (Freeman, New York, 1985).
3. O. Eugster, *Science* **245**, 1197 (1989).
4. C. Koeberl and W. A. Cassidy, *Lunar Planet. Inst. Tech. Rep. 90-01* (1990).
5. J. E. Dennison and M. E. Lipschutz, *Geochim. Cosmochim. Acta* **51**, 741 (1987).
6. J. T. Wasson *et al.*, *ibid.* **53**, 735 (1989).
7. J. T. Wasson, *Science* **249**, 900 (1990).
8. E. Jarosewich, *Lunar Planet. Inst. Tech. Rep. 90-01* (1990), p. 54.
9. H. Takeda, *ibid.*, p. 86.
10. G. W. Wetherill, *Meteoritics* **20**, 1 (1985).
11. D. W. G. Sears, *Nucl. Tracks Radiat. Meas.* **14**, 5 (1988).
12. M. Haq, F. A. Hasan, D. W. G. Sears, *Geochim. Cosmochim. Acta* **52**, 1679 (1988).
13. K. Nishiizumi, D. Elmore, P. W. Kubik, *Earth Planet. Sci. Lett.* **93**, 299 (1989).
14. P. H. Benoit, H. Sears, D. W. G. Sears, *J. Geophys. Res.*, in press.
15. D. W. G. Sears, P. Benoit, J. D. Batchelor, *Geochim. Cosmochim. Acta* **55**, 1193 (1991).
16. L. Schultz, H. W. Weber, F. Begemann, *ibid.*, p. 59.
17. J. A. Wood, *Icarus* **6**, 1 (1967).
18. K. Nishiizumi, S. Regnier, K. Marti, *Earth Planet. Sci. Lett.* **50**, 156 (1980).
19. J. Willis and J. I. Goldstein, *Proc. Lunar Planet. Sci. Conf.* **12**, 1135 (1981).

20. We thank the U.S. Antarctic Meteorite Working Group and M. E. Lipschutz for samples and documentation, J. Roth and V. Yang for technical assistance, and G. A. McKay for access to the Johnson Space Center electron microprobe. This research was supported by National Aeronautics and Space Administration grant NAG 9-81 and National Science Foundation grant DPP 86-13998.

15 November 1991; accepted 31 January 1992

Response of Regional Seismicity to the Static Stress Change Produced by the Loma Prieta Earthquake

PAUL A. REASENBERG AND ROBERT W. SIMPSON

The 1989 Loma Prieta, California, earthquake perturbed the static stress field over a large area of central California. The pattern of stress changes on major faults in the region predicted by models of the earthquake's dislocation agrees closely with changes in the regional seismicity rate after the earthquake. The agreement is best for models with low values of the coefficient of friction ($0.1 \leq \mu \leq 0.3$) on Bay Area faults. Both the stress models and measurements suggest that stresses were increased on the San Andreas fault north of the Loma Prieta rupture, but decreased slightly on the Hayward fault. This relaxation does not warrant lower probability estimates for large earthquakes on the Hayward fault in the next 30 years, however.

THE MAGNITUDE (M) 7.1 LOMA PRIETA earthquake was the largest earthquake to strike the San Francisco Bay region since 1906 (*1*). In addition to radiating seismic waves, the earthquake introduced a static stress perturbation to the region as a result of its displacement, which averaged about 2 m between depths of 6 and 18 km. An immediate concern after the earthquake was the possible effect this stress perturbation might have had on other major faults in the Bay Area. On two occasions in the 1800s a large earthquake on one side of the Bay had been followed within 3 years by a second large earthquake on the opposite side (*2*). Because the Hayward fault probably ruptured on both of these occasions, the stress changes on the Hayward fault were of particular interest (*3*). To evaluate the possibility of such interactions we determined the static stress changes produced within an elastic half space by model dislocation surfaces, and compared the results to regionally observed changes in the rates of seismicity (*4, 5*).

For our stress calculations we simulated the Loma Prieta displacement at depth by a rectangular dislocation surface inferred from geodetic measurements made before and after the earthquake (*6*). Although complexities in the seismic waveforms observed during the earthquake suggest that the rupture was complex (*7*), we chose to use a simple model for initial calculations; our calculated results are least accurate in the near field (within about 40 km of the rupture surface) where the details of the slip distribution are important. In the far field, the details of the slip distribution become less important than the total moment of the earthquake and the average orientation of the rupture plane.

The major faults in the Bay Area were represented by alignments of vertical 10-km-long rectangular patches extending from the surface to a depth of 13 km (*8*). Stress changes were calculated at the centers of the patches (*9*). Both shear stress and normal stress changed on the fault surfaces as a result of the Loma Prieta earthquake. Because the major vertical Bay Area faults are probably loaded predominantly by right-lateral shear, the shear stress changes imposed by the Loma Prieta rupture can either increase (if the change is right-lateral) or decrease (if the change is left-lateral) the shear load. Laboratory studies of rock friction and failure suggest that normal forces are important in determining resistance to sliding (*10*). We defined a Coulomb failure function (*CFF*) for comparison with changes in rates of seismicity:

$$CFF \equiv |\tau| - \mu(\sigma - p) - S$$

This function is based on the Coulomb criterion for shear failure of rocks

$$|\tau| \geq \mu(\sigma - p) + S$$

where $|\tau|$ is the magnitude of shear traction acting on the plane, σ is the normal traction (positive for compression), p is the pore fluid pressure, μ is the coefficient of internal friction, and S is the cohesion (*11*). Thus changes in the *CFF* are given by

$$\Delta CFF = |\tau| - |\tau_0| - \mu(\Delta\sigma - \Delta p) - \Delta S$$

This expression is nonlinear in the changes in shear stress (*12*). It can be simplified by assuming that for vertical strike-slip faults the horizontal shear stresses are most important and that changes are superposed on a preexisting background level of right-lateral shear for most faults in the Bay Area. This leads to

$$\Delta CFF \approx \Delta\tau_{hrl} - \mu\Delta\sigma$$

where $\Delta\tau_{hrl}$ is the change in horizontal component of right-lateral shear stress (positive for more right-lateral) and $\Delta\sigma$ is the change in normal stress (positive for more compression) (*13*). We also assume here that changes in p and S are negligible.

As discussed below, a choice of $\mu = 0.2$ yielded the best agreement with observed seismicity rate changes (Fig. 1). Changes in *CFF* ranged from a few bars to less than 0.01 bar (Fig. 1). San Andreas fault segments at either end of the Loma Prieta

U.S. Geological Survey, Mail Stop 977, 345 Middlefield Road, Menlo Park, CA 94025.

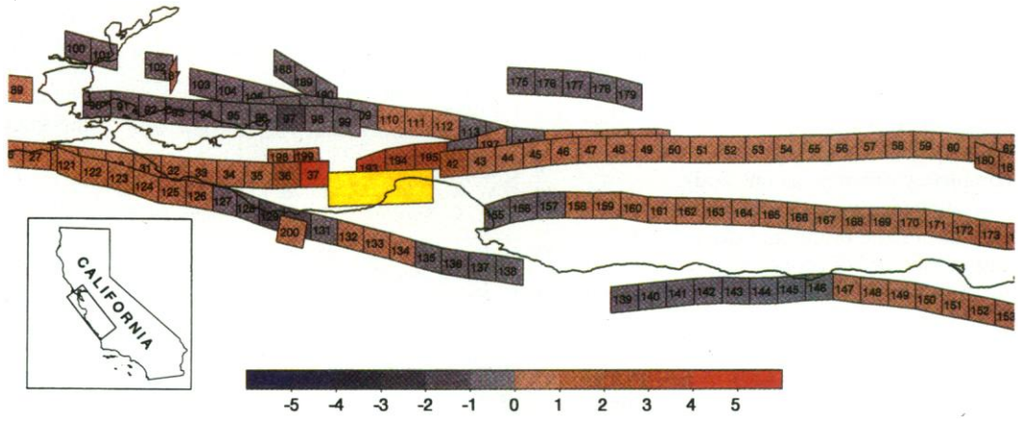

Fig. 1. Static stress changes produced by the Loma Prieta earthquake on vertical planar segments representing faults in central California, calculated using an elastic model with a rectangular dislocation (yellow) derived from geodetic measurements. Change in the Coulomb failure function ΔCFF (in bars) on each fault segment for $\mu = 0.2$ is indicated by color. Segments with increased *CFF* (red) are more likely to produce earthquakes; segments with decreased *CFF* (blue), less likely. This oblique view is from the southwest and down at an angle of 45°. Inset map shows study area. Segment numbers are shown for reference in Fig. 3.

rupture are closer to failure than before the rupture because of the additional right-lateral stress loaded onto them. Estimates from similar models of the time by which these stress changes might advance the occurrence of the next earthquakes on segments to the north of the Loma Prieta rupture range from 2 to 25 years (*3*). On the Hayward fault, changes in *CFF* range from 0.03 bar at the north end to 0.8 bar at the south end, in a sense to delay the onset of the next earthquake. For a long-term slip rate of 9 mm/year these changes in *CFF* amount to delays ranging from less than 1 to 10 years, although these static, purely elastic models may poorly estimate the longer term effect (*14*).

In order to see if any of these stress changes were reflected in seismicity, we measured the regional coseismic change in seismicity rate using the statistic β, which is sensitive to a contrast of average seismicity rate between two time intervals in a specified area (*15*). We compared the rate r_a in the postseismic interval of duration t_a with the rate r_b in the preseismic interval of duration t_b, where $r_a = n_a/t_a$, $r_b = n_b/t_b$, and n_a, n_b are the numbers of earthquakes occurring in the respective intervals. The rate change is expressed as

$$\beta(n_a, n_b, t_a, t_b) = \frac{n_a - E(n_a)}{\sqrt{var(n_a)}}$$

where *var* denotes variance and $E(n_a) = r_b t_a$ is the value of n_a expected under the null hypothesis of stationary random occurrence (*16*). We calculated β for fixed t_a and t_b in overlapping 10-km-square cells covering an area 140 by 390 km for the preseismic (background) period between 17 October 1979 and 17 October 1989 and postseismic period between 18 October 1989 and 31 May 1991 (*17–19*) (Fig. 2). Positive values of β indicate that the postseismic rate was higher than the background rate; negative values, lower (*20*). A symmetry in the definition of β introduces an ambiguity in interpretation, whereby a relatively low postseismic rate cannot be distinguished from an abnormally high preseismic rate, as would result, for example, from an earthquake swarm or aftershock sequence in the preseismic (background) period. Several such artifacts corresponding to the aftershocks of moderate earthquakes in the region in the pre–Loma Prieta background period initially were detected with the complete catalog. To reduce these effects, we removed aftershocks from the catalog with a computer algorithm (*21, 22*).

Areas of high postseismic seismicity rate include the immediate aftershock zone (from Los Gatos to Watsonville); the San Francisco Peninsula in an area of thrust faults near Los Gatos and along the San Andreas and San Gregorio faults near Daly City; along the San Andreas and Sargent faults from Watsonville to Bear Valley; a partially offshore segment of the San Gregorio fault near Point Ano Nuevo; and along the Alamo fault, near Livermore. With the exception of the activity near Point Ano Nuevo (*23*), these areas generally coincide with fault segments having increased *CFF*. Areas of apparent coseismic decrease in seismicity rate occur along the southern Calaveras, Hayward, southern Rodger's Creek, and Mount Lewis faults; these fault segments also have relaxed stress ($\Delta CFF < 0$). Other aftershock sequences before 1989

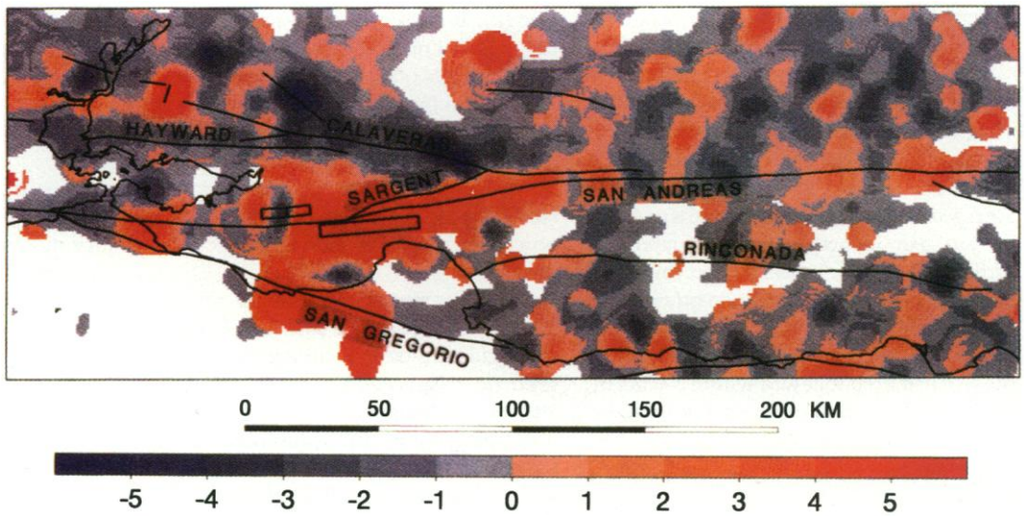

Fig. 2. Changes in seismicity rate β in central California occurring at the time of the Loma Prieta earthquake. Values of β (color) compare average rates in the intervals 17 October 1979 to 17 October 1989 and 18 October 1989 to 30 June 1991. Areas that experienced a coseismic increase (decrease) in seismicity rate are shown as red (blue); areas with insufficient earthquakes for determination of β are white. Absolute value of β indicates the statistical significance of the rate change, taking into account the variance of the background seismicity. Major faults and coastline are indicated by solid lines.

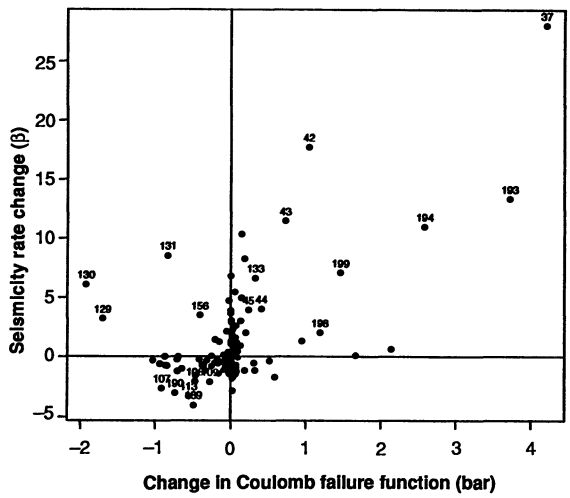

Fig. 3. Seismicity change β and stress change $\Delta CFF(\mu)$ on 141 model fault segments for $\mu = 0.2$. Numbers (refer to Fig. 1) indicate segments experiencing the largest changes ($|\overline{\beta}_j| \geq 2$ and $|\Delta CFF_j| \geq 0.2$ bar).

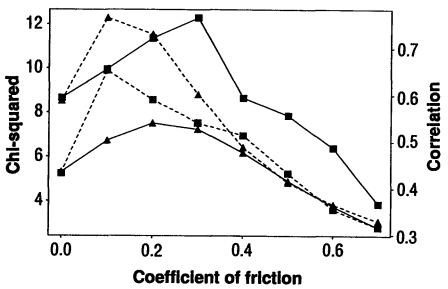

Fig. 4. Measures of agreement between stress changes and seismicity changes on fault segments, shown as a function of the coefficient of friction μ. Squares, values of χ^2 (scale on left); triangles, coefficients of correlation between stress change and seismicity change (scale on right). Solid lines, all 141 fault segments; broken lines, fault segments experiencing significantly large changes (numbered points in Fig. 3). Chi-squared confidence levels are 6.64 ($p = 0.01$) and 10.83 ($p = 0.001$).

preclude unambiguous interpretation of the negative values of β observed along the southern Calaveras and Mount Lewis faults in terms of postseismic effects. The Hayward fault, however, was essentially free of significant swarm and aftershock activity during the 1980s. Consequently, the apparent low postseismic rate observed there (strongest on the southern Hayward fault) is not believed to be an artifact and may be related to the Loma Prieta earthquake.

To investigate the overall dependence between the modeled stress changes and the observed seismicity, we compared, for each fault segment S_j, the mean seismicity rate change index $\overline{\beta}_j$ corresponding to the subset of cells within 5 km of segment S_j to the coseismic static stress change $\Delta CFF_j(\mu)$ calculated on that segment, for various assumed values of the coefficient of friction μ (*24*). We show one of the better fitting comparisons (for $\mu = 0.2$) in Fig. 3. For this value of μ, concordant changes in stress and seismicity (both increase or both decrease) occurred on 87 fault segments, discordant changes occurred on 54 segments, and a generally positive correspondence between $\overline{\beta}$ and ΔCFF is visually apparent. A χ^2 test on all fault segments rejects the null hypothesis that $\overline{\beta}$ and $\Delta CFF(\mu)$ are independent ($p < 0.001$ for $0.2 \leq \mu \leq 0.3$; $p < 0.01$ for $0.1 \leq \mu \leq 0.4$) (*25*). The correlation coefficient ρ attains its maximum value for $\mu = 0.2$, and exceeds 0.5 for $0.1 \leq \mu \leq 0.3$ (Fig. 4) (*26*).

Static stress changes as small as a few tenths of a bar apparently produced detectable changes in seismicity. This level of stress change is about one order of magnitude larger than that of tidally induced stress changes (*27*), and is comparable to stress changes produced at seismogenic depths by the filling of water reservoirs (*28*). The response of seismicity to stress change decreases with distance from the dislocation, and is statistically undetectable (at the $p = 0.05$ level) at distances beyond 80 to 100 km; at this distance the maximum absolute value of ΔCFF is approximately 0.1 bar (*29*). The apparent sensitivity of regional seismicity to such small stress changes suggests that fluctuations in regional seismicity may be used to detect and model some aseismic slip events, including afterslip, slow earthquakes, slip on the ductile portion of vertical faults, and slip on horizontal detachment surfaces.

Our observations of the regional seismicity response to the Loma Prieta earthquake favor models involving low friction ($0.1 \leq \mu \leq 0.3$) on central California faults. In contrast, laboratory experiments on frictional slip in rock that typically have indicated higher coefficients of friction ($0.5 \leq \mu \leq 0.8$) have been widely used as an analog for brittle faulting in the upper 15 to 20 km of the crust (*30*). Our result is consistent with the idea that low friction could explain seismological and other evidence for fault-normal compression in central California (*12, 31*) and the lack of an observable heat flow anomaly associated with the San Andreas fault (*32*). The apparent low friction value could also be explained by a high coefficient of friction (consistent with laboratory studies) combined with changes in pore pressure in a compliant fault zone (*33*).

Our observations support the conclusion (*3*) (based on stress models alone) that sections of the San Andreas fault north of the Loma Prieta earthquake were probably moved closer to failure as a result of the stress change produced by the earthquake. In addition, the Hayward fault may have relaxed slightly. Such relaxation may be only temporary, however. Simple models suggest that nonelastic adjustments and continued loading with time may alter both the magnitude and sign of stress changes induced on other faults by the Loma Prieta earthquake (*34*). The minimal degree of relaxation, uncertainties in its estimation, and its temporary effect offer no basis for reducing the 30-year probabilities for large earthquakes in central California or the regional efforts to prepare for them.

Our result suggests that the Loma Prieta earthquake will not trigger an earthquake on the Hayward or Mission fault. This conclusion, however, relies on a simple structural model consisting of vertical faults. The presence of dipping structures along the Hayward fault could change this result (*35*). Some of our models with nonvertical Hayward and Mission faults weakly support a triggering hypothesis, but these are poorly constrained by or inconsistent with the seismicity (*36*). If such a pairing does occur, however, it would suggest that our present structural model is inadequate or that nonelastic effects have exceeded the static elastic stress changes, or both.

REFERENCES AND NOTES

1. U.S. Geological Survey Staff, *Science* **247**, 286 (1990).
2. The 1836 ($M \sim 6.8$) earthquake on the northern Hayward fault was followed in 1838 by an ($M \sim 7.0$) earthquake on the San Francisco Peninsula section of the San Andreas fault, and the 1865 ($M \sim 6.5$) earthquake, possibly on the Loma Prieta segment of the San Andreas fault, was followed in 1868 by an ($M \sim 7.0$) earthquake on the (possibly southern) Hayward fault [W. L. Ellsworth, *U.S. Geol. Surv. Prof. Pap. 1515* (1990), p.153].
3. Working Group on California Earthquake Probabilities, *U.S. Geol. Surv. Circ. 1053* (1990). The working group considered in detail the effect of an increase in right-lateral shear stress on segments of the San Andreas fault north of the Loma Prieta earthquake rupture. They concluded that the effect was to shorten the time to the next earthquake on these segments.
4. Other studies have suggested that changes in static stress might affect patterns or focal mechanisms of aftershocks or trigger other earthquakes. These include R. S. Stein and M. Lisowski, *J. Geophys. Rev.* **88**, 6477 (1983); G. M. Mavko, S. Schultz, B. D. Brown, *Bull. Seismol. Soc. Am.* **75**, 475 (1985); L. Erickson (*5*); D. H. Oppenheimer *et al.* (*12*); C. M. Poley, A. G. Lindh, W. H. Bakun, S. S. Schulz, *Nature* **327**, 134 (1987); K. W. Hudnut, L. Seeber, J. Pacheco, *Geophys. Res. Lett.* **16**, 199 (1989); P.

A. Rydelek and I. S. Sacks, *Geophys. J. Int.* **100**, 39 (1990); L. Seeber and J. G. Armbruster, *Geophys. Res. Lett.* **17**, 1425 (1990); A. J. Michael, W. L. Ellsworth, D. O. Oppenheimer, *ibid.*, p. 1441; A. J. Michael, *J. Geophys. Res.* **96**, 6303 (1991).
5. L. Erickson, thesis, Stanford University (1986).
6. M. Lisowski, W. H. Prescott, J. C. Savage, M. J. Johnston, *Geophys. Res. Lett.* **17**, 1437 (1990). The model dislocation strikes at N44W, dips 70SW, extends 37 km horizontally, has its top at a depth of 5 km and its bottom at a depth of 17.5 km. Right-lateral slip of 1.66 m and reverse slip of 1.19 m yield a moment of 3.0×10^{19} N · m for this model. More complex models of the rupture were also used to predict the static stress changes. Although the results with these models vary in their details, our overall result is apparently not sensitive to the choice of rupture model.
7. See, for example, G. Beroza, *Bull. Seismol. Soc. Am.* **81**, 1603 (1991).
8. In addition, two nonvertical fault segments (198 and 199) were included, representing dipping thrust planes northeast of the San Andreas fault near Los Gatos. A third dipping plane (200) adjacent to the San Gregorio fault was not used in the statistical evaluation, but was added for illustrative purposes [see (*23*)].
9. The depth of the segment centers (6.5 km) coincides with the median depth of seismicity used in this study.
10. J. D. Byerlee, *Pure Appl. Geophys.* **116**, 615 (1978).
11. J. C. Jaeger and N. G. W. Cook, *Fundamentals of Rock Mechanics* (Chapman and Hall, ed. 3, London, 1979).
12. D. H. Oppenheimer, P. A. Reasenberg, R. W. Simpson, *J. Geophys. Res.* **93**, 9007 (1988).
13. For the two dipping fault segments (198 and 199) representing reverse faults, ΔCFF was calculated for the assumption that the dominant shear stress on these planes before the Loma Prieta earthquake was oriented up-dip in a thrust sense.
14. The ranges in these estimates reflect the range in distance of the segments from the Loma Prieta earthquake and uncertainty about rates of loading and magnitudes of earlier earthquakes on these fault segments. No evidence currently justifies estimating the time of advance or delay of the next large earthquake from the modeled average static stress change on a fault. The earthquake process and crustal structure are complex, and the existence of a simple relation between stress change and time to the next large earthquake is as yet unproved.
15. M. V. Matthews and P. A. Reasenberg, *Pure Appl. Geophys.* **126**, 357 (1988). The rate change index β is defined with respect to the null hypothesis, which states that the earthquake occurrence has a Poissonian distribution with the postseismic rate equal to the background rate.
16. The variance was represented by that of a binomial process: $var(n_a) = n_b t_a$.
17. We used $M \geq 1.5$ earthquakes in the U.S. Geological Survey central California catalog.
18. The period 1979 to 1989 produced an unusually large number of ($M \geq 5$) earthquakes in central California, including the 1979 Coyote Lake (M = 5.9), 1980 Livermore (M = 5.9), 1983 Coalinga (M = 6.7), 1984 Morgan Hill (M = 6.2), 1985 Kettleman Hills (M = 5.5), 1986 Mount Lewis (M = 5.7), 1986 Quien Sabe (M = 5.7), 1986 Alum Rock (M = 5.3), and the 1988 and 1989 Lake Elsman (M = 5.0, M = 5.2) earthquakes. This series of earthquakes has been interpreted as possible evidence of an intermediate-term precursory process leading to the Loma Prieta earthquake [L. R. Sykes and S. C. Jaume, *Nature* **348**, 595 (1990)].
19. The background periods 17 October 1969 to 17 October 1979 and 17 October 1969 to 17 October 1989 were also tried, and similar results were obtained. Because of improved stability of the network, the background period 1979 to 1989 is considered most reliable.
20. Significance levels for $|\beta|$ estimated from its asymptotic (Gaussian) distribution are 1.96 (p = 0.05) and 2.57 (p = 0.01).
21. P. A. Reasenberg, *J. Geophys. Res.* **90**, 5479 (1985). Results presented in this paper are based on analysis of the catalog with aftershocks removed. Removal of aftershocks reduced (but did not completely eliminate) these artifacts. The low apparent postseismic rate ($-3 \leq \beta < 0$) remaining in some of these areas (for example, along the Calaveras and Mount Lewis faults) still hampers interpretation of these features as postseismic effects.
22. Apparent changes in seismicity rate may result from man-made factors, including changes in network operations and method used to calculate earthquake magnitude. R. E. Habermann and M. S. Craig [*Bull. Seismol. Soc. Am.* **78**, 1225 (1988)] suggested the presence of such shifts in the catalog during the 1970s. However, because the period 1984 to 1991 is believed to be free of such effects [D. Oppenheimer, personal communication], we do not believe that the seismicity changes we observed are significantly affected by such artifacts.
23. Segments 129, 130, and 131 experienced sizable seismicity rate increases and calculated decreases in $CFF(\mu)$ for all values of friction (see Fig. 3). However, as illustrated by the dipping segment (200) adjacent to segment 130, thrust mechanisms would be favored in this vicinity. Furthermore, earthquake focal mechanism solutions suggest that a majority of the earthquakes there were oblique right-lateral thrust events on dipping planes.
24. We used values of β obtained with aftershocks removed for the background period 1979 to 1989.
25. Evaluation of a fourfold table with a two-sided χ^2 test was carried out on 141 segments. Significance levels for χ^2 are 3.84 (p = 0.05), 6.64 (p = 0.01) and 10.83 (p = 0.001) [see, for example, L. Sachs, *Applied Statistics* (Springer-Verlag, New York, 1982), pp. 346–351].
26. Many of the points in Fig. 3 indicate absolute changes in stress or seismicity on individual segments comparable to the uncertainties associated with modeling errors (stress) and stochastic variance (seismicity). When these tests were applied to a subset of fault segments with significant changes in stress and seismicity (numbered points in Fig. 3), similar results were obtained. χ^2: $p < 0.01$ for $0.1 \leq \mu \leq 0.4$; correlation: ρ exceeds 0.5 for $0.0 \leq \mu \leq 0.3$.
27. T. H. Heaton, *Bull. Seismol. Soc. Am.* **72**, 2181 (1982); M. McNutt and T. H. Heaton, *Calif. Geol.* **34**, 12 (1981); F. D. Stacey, *Physics of the Earth* (Wiley, ed. 2, New York, 1977).
28. E. A. Roeloffs, *J. Geophys. Res.* **93**, 2107 (1988).
29. Using μ = 0.2 we calculated χ^2 for subsets of segments in various ranges of distance from the center of the earthquake dislocation. χ^2 is maximum ($\chi^2 > 21$) for the 80 segments between 0 and 100 km from the source; χ^2 just fails to exceed the p = 0.05 critical point for the farthest 70 segments located 80 or more km from the earthquake.
30. See, for example, J. D. Byerlee and W. F. Brace, *J. Geophys. Res.* **73**, 6031 (1968) and J. H. Dieterich, in *Mechanical Behavior of Crustal Rocks*, N. Carter, M. Friedman, J. Logan, D. Stearns, Eds. (American Geophysical Union, Washington, DC, 1981), pp. 103–120.
31. M. D. Zoback *et al.*, *Science* **238**, 1105 (1987), and references therein.
32. A. H. Lachenbruch and A. McGarr, *U.S. Geol. Surv. Prof. Pap.* **1515**, 261 (1990).
33. For discussions of pore pressure effects see, for example, J. Byerlee, *Geophys. Res. Lett.* **17**, 2109 (1990); J. R. Rice, in *Fault Mechanics and Transport Properties of Rock*, B. Evans and T.-F. Wong, Eds. (Academic Press, London, in press).
34. M. F. Linker and J. R. Rice, *Eos* **72**, 310 (1991).
35. The presence of a buried thrust under the Mission fault was suggested by D. J. Andrews, *Eos* **72**, 446 (1991). Also see R. S. Stein and G. C. P. King, *Science* **224**, 869 (1984); D. L. Jones, A. J. H. Lomax, T. V. McEvilly, *Eos* **72**, 446 (1991).
36. W. L. Ellsworth, J. A. Olson, L. N. Shijo, S. M. Marks, *Calif. Div. Mines Geol., Spec. Publ. 62* (1982).
37. We thank R. Archuleta, W. Ellsworth, A. Lindh, M. Linker, A. Michael, D. Oppenheimer, J. Rice, and P. Segall for helpful discussion and comments and thoughtful reviews of the manuscript.

22 November 1991; accepted 3 February 1992

The Fossil Record and Evolution: Comparing Cladistic and Paleontologic Evidence for Vertebrate History

MARK A. NORELL AND MICHAEL J. NOVACEK

The fossil record offers the only direct evidence of extinct life and thus has figured prominently in considerations of evolutionary patterns. But the incomplete nature of the fossil record has also been emphasized in arguments that fossils play only a secondary role in the recovery of phylogenetic histories based on extant taxa. Although these criticisms recently have been countered, there is no general understanding of the correspondence between the fossil record and phylogeny. An empirical survey of recently published studies suggests no basis for assuming that the stratigraphic occurrence of fossils always provides a precise reflection of phylogeny. Nevertheless, our survey of a sample of taxa shows a tendency for positive correlation between age and clade rank and, hence, a degree of correspondence between phylogenetic pattern and the paleontologic record.

SINCE THE BIRTH OF PALEONTOLOGY the fossil record has been interpreted as a record of life's history. The paleontologic record of horses, for example, has been claimed to demonstrate the potential of fossils in disclosing the branching sequence of taxa through time as well as indicating major evolutionary trends toward increasing specializations (*1–3*). However, what patterns do this record reflect and how precisely do they capture evolutionary events? For instance, fossils have been considered to provide so little evidence for relationships among living taxa that it has been suggested that they be relegated to a secondary role in reconstruction of phylogeny (*4–6*). Such criticisms and recommendations are countered in a recent demonstration that fossil taxa preserve pivotal evidence for ancient

Department of Vertebrate Paleontology, American Museum of Natural History, New York, NY 10024.